

Magnetic Resonance Imaging in Neurologic Diseases

—Comparison with Computed Tomography—

Kee Hyun Chang, M.D., Man Chung Han, M.D. and Chu Wan Kim, M.D.

Department of Radiology, College of Medicine, Seoul National University, Seoul, Korea

Magnetic resonance (MR) and computed tomography (CT) imagings were compared in 121 patients with various neurologic diseases. MR was performed with either 0.15 Tesla resistive or 2.0 Tesla superconducting systems developed by Korea Advanced Institute of Science and Technology (KAIST), using multi-slice spin echo technique with a variety of pulse sequences reflecting proton density, T1 and T2 relaxation times. MR was more advantageous in the detection of the lesions, accurate depiction of the lesion extents, and/or demonstration of anatomic details in sagittal or coronal plane in 36 of the 121 patients. These included white matter diseases, cervical cord tumors, syringomyelia, brain stem tumors, foramen magnum tumor, acute cerebellar infarction, Chiari malformation, isodense subacute subdural hematomas, cavernous hemangioma, A-V malformation with hemorrhage and some unknown pathologies.

Even though 2.0T superconducting system showed greater capability of demonstrating the anatomic details and contrast discrimination between normal and abnormal tissues, the ability of MR to separate the tumor from the edema and to differentiate among different pathologic entities remained to be further evaluated. CT was superior to MR in 13 patients with acute intracranial hematomas, small calcific lesions, inflammatory granulomas or meningiomas. CT takes less time and may be preferable in very young or elderly patients. Both MR and CT gave equivalent information in the remaining patients. MR proved to complement CT in the evaluation of many disease entities and may actually supplant CT in some.

Key Words: *Magnetic Resonance Imaging, MR, Neurologic Disease, CT*

INTRODUCTION

Clinical experience with MR imaging, particularly of the brain, has been rapidly accumulating. The diagnostic superiority of MR over computed tomography has already been shown for various con-

ditions (Bydder et al., 1982; Brant-Zawadzki et al., 1983; Bradley et al., 1984; Han et al., 1984). However, current MR equipment and technology are still developing and not completely standardized. Both hardware and imaging technique differ substantially among the imagers now being used.

Certain techniques are already proving more useful than others in delineating pathology (Brant-Zawadzki et al., 1983). Because of the rapidly changing technology, clinical efficacy questions regarding MR are still somewhat premature.

Comparison studies with CT must be evaluated

Address for Correspondence: Dr. Kee Hyun Chang, Dept. of Diagnostic Radiology, Seoul National University Hospital, Yeonkun-Dong 28, Chongno-Ku, Seoul 110, Korea.

This study was supported in part by special research fund of Seoul National University Hospital (1986).

with the understanding that one is comparing the technologies at very different stages of maturity.

This report describes our experience with MR developed by Korea Advanced Institute of Science and Technology for the evaluation of 121 patients with suspected neurologic diseases and compares the MR data with CT findings in an effort to define the role of MR in evaluating CNS pathology.

SUBJECTS AND METHODS

We retrospectively reviewed the cerebral and upper cervical MR images of 121 patients (Table 1) examined with either 0.15 Tesla resistive or 2.0 Tesla superconducting system, which were developed by KAIST. One hundred-six patients were

studied with 0.15 Tesla resistive system at either KAIST or Shinwha Hospital over a 20-month period, and the remainder was examined with 2.0 Tesla prototype at KAIST over the past 6 months. These patients had been referred for MR on the basis of either CT study, or symptoms and signs suggestive of neurological disorder. Most of the patients had a firm diagnosis based on clinical, CT and/or pathologic biopsy criteria. The age of the patients ranged from 2 to 75 years. Seventy-two patients were male and 49 were female.

Thirteen patients who had either suspicious CT findings, or clinical suspicion of neurological disease but showed normal MR features were included in the present study and categorized into "normal" group. Forty-four patients had various

Table 1. Case distribution

Diagnosis	Case No.	Diagnosis	Case No.	Total 121 (15)
Normal	13 (1)	cerebellar medulloblastoma	1	
Hemorrhage	7	foramen magnum meningioma	1 (1)	
Acute epidural hematoma (EDH)	1	Cervical cord		
Acute intracerebral hematoma (ICH)	1	cervical cord tumor	3	
Acute intraventricular hematoma (IVH)	1	syringomyelia	4 (3)	
Acute ICH with A-V malformation	1	Unknown	9	
Subacute ICH & subdural hematoma (SDH)	1	Inflammation	16 (3)	
Subacute isodense SDH	1	Cysticercosis	11 (3)	
Chronic SDH	1	Granuloma	4	
Infarction	5 (1)	Sphenoid pyomucocele	1	
Cerebral infarction	3	Demyelinating & Degenerative diseases	28 (4)	
Cerebellar infarction	2 (1)	CO poisoning	11 (1)	
Neoplasm	44 (4)	Subcortical atherosclerotic encephalopathy (SAE)	4 (1)	
Supratentorial		Multiple sclerosis	1	
glioma	5	Adrenoleukodystrophy	1	
meningioma	2	Radiation necrosis	1	
germinoma	1	Wilson's disease	1	
cavernous hemangioma	1	Parkinsonism	1	
Sellar & Juxtaseilar		Olivopontocerebellar atrophy (OPCA)	2 (1)	
pituitary adenoma	2	Unknown	6 (1)	
craniopharyngioma	2	Congenital anomalies	3	
epidermoid	2	Chiari malformation	1	
germinoma	1	Ependymal cyst	1	
solidly enhancing tumor	1	Arachnoid cyst	1	
Infratentorial		Miscellaneous	5 (2)	
brainstem tumor	4	Hydrocephalus	2	
acoustic neurinoma	4	Vertebral disease	2 (2)	
cerebellar metastasis	1	Scalp lipoma	1	

* Number in Parenthesis: Case number examined with 2.0T unit.

kinds of tumors in the brain and upper cervical cord. Sixteen patients had inflammation including cysticercosis and inflammatory granuloma. Twenty-eight patients had demyelinating and/or degenerative diseases. The remainder includes 7 cases of hemorrhages, 5 cases of ischemic infarcts, 3 cases of congenital anomalies and 5 miscellaneous cases.

The MR studies were performed using multi-slice spin echo (SE) technique with a variety of pulse sequences reflecting proton density, T1 or T2 relaxation times. The spin-echo sequence (90°-180°) generated images at echo times (TE) of 30, 60, 80, 90 or 120 msec. Repetition times (TR) of 0.4, 0.5, 0.9, 1.5, or 2.0 seconds were used, depending on the clinical presentation and suspected pathology. The routine MR evaluation was performed with a TR/TE of 400/30 and 900/60 or 1200/90 msec with 0.15T unit, and with a TR/TE of 500/30 and 2000/80 msec with 2.0T unit. Inversion recovery (IR) imaging was seldom used. A two-dimensional Fourier transform was employed. Multi-slice acquisition permitted up to 10 to 20 sections to be generated in the pulse sequence with long TR and 6 slices with short TR. A 256 x 256 acquisition matrix was used, corresponding to spatial resolution of 1.0mm. The slice thickness and interval were usually 1cm. Four to six repetitions were made with 0.15T unit, taking a total of 10 to 20 minutes, but 2 averages were made with 2.0T unit, taking less time. Imaging was performed in the axial, coronal and/or sagittal plane, depending on the cases. But most known or suspected lesions were imaged only in the axial plane.

A brain CT scan was available for each patient evaluated with MR. Most of the CT scans were obtained within two weeks of the MR study using GE 8800 unit. The CT scans employed continuous 10mm sections and post-contrast scan in most of the cases. The MR and CT findings were compared in each case.

RESULTS

MR Features

Normal MR studies (13 cases)

Normal MR images were obtained in cases of clinically suspected vertebrobasilar insufficiency (four cases), multiple sclerosis (four) and brainstem lesion (three). No abnormality was demonstrated on CT in any of these cases. The other two patients with suspicious abnormal findings on CT also re-

vealed no abnormality in MR images.

Intracranial Hemorrhages (7 cases)

Two cases of 4 acute intracranial hemorrhages (one hypertensive hemorrhage in basal ganglia and one traumatic epidural hematoma) were studied with only SE 400/30 technique and other 2 acute cases (one intracerebral hemorrhage secondary to rupture of arteriovenous malformation (AVM) and one intraventricular hematoma) were examined with only T2-weighted SE (SE 1200/60). The hematomas in these cases revealed isosignal or slightly high signal intensity on SE 400/30 but much higher signal intensities on SE 1200/60 images. In an epidural hematoma case, the dura mater between the brain parenchyme and the hematoma was well visualized as a curvilinear low intensity. The AVM case showed feeding arteries and draining veins of low intensity in the vicinity of the hematoma. Like the CT, the mass effect was well demonstrated. In a case with both intracerebral (ICH) and subdural hematomas examined 2 weeks after head trauma, uniform high signal intensity lesions were clearly demonstrated on SE 1200/60, but peripheral rim of high signal intensity and central region of isosignal intensity was shown in ICH on SE 400/30. In 4 weeks follow-up study, the isosignal intensity of central region was changed to slightly higher signal intensity on SE 400/30. One case with bilateral isodense subdural hematoma on CT revealed slightly low signal intensity and striking high signal intensity on SE 400/30 and 900/60, respectively. Another case of chronic subdural hematoma showed low signal intensity same as that of CSF on SE 400/30.

Ischemic infarctions (5 cases)

All the 5 cases of acute or subacute infarction revealed high signal intensity on T2 weighted SE (SE 900/60, 1200/90 or 2000/80), while 3 of the 5 cases showed low signal intensity and two showed isosignal intensity on SE 400/30. On IR studied in 3 cases the infarcts showed low signal intensities.

Neoplasms (44 cases)

Nine cases of supratentorial tumors (5 gliomas, 2 meningiomas, 1 germinoma, 1 cavernous hemangioma), 8 cases of sellar and parasellar tumors (2 pituitary adenomas, 2 craniopharyngiomas, 2 epidermoids, 1 germinoma, 1 solidly enhancing tumor), 11 cases of infratentorial tumors (4 brainstem tumors, 4 acoustic neurinomas, 1 cere-

bellar metastasis, 1 medulloblastoma, 1 foramen magnum meningioma), 7 cervical cord tumors (including 4 syringomyelias) and 9 unknown tumors were examined.

All the cases demonstrated the lesion on both MR and CT.

Solid components of the supratentorial gliomas, brainstem tumors, cervical cord tumors, meningiomas, acoustic neurinomas, pituitary adenomas, germinomas, metastasis and medulloblastoma were seen as slightly low-intensity or iso-intensity areas on SE 400/30 and as high-intensity areas on SE 900/60, SE 1200/60, SE 1500/90 or SE 2000/80. It was difficult to separate the tumors from the surrounding edema, and to differentiate among the different pathologic entities even with 2.0T unit. But on the SE 1200/90 images of the meningiomas, the round well-outlined tumors with slightly high-intensity could be readily differentiated from the surrounding edema with much higher intensity. One germinoma and one cavernous hemangioma showed small areas of high intensity within the isodense tumors on SE 400/30, which suggested hemorrhagic foci within the tumors.

The cystic or necrotic portions of the gliomas, syrinx cavities, and epidermoids revealed same intensity as those of CSF on both SE 400/30 and SE 900/60 or SE 1200/90 images; They showed low signal intensity on SE 400/30, and high signal intensity on SE 1200/90. Curvilinear vascular structures within the cavernous hemangioma was well seen as low intensity on both SE 400/30 and SE 900/60. Two craniopharyngiomas showed high intensity on both SE 400/30 and SE 900/60. Nine unknown cases revealed low signal or isosignal intensity on SE 400/30 and high signal intensity on SE 900/60 and/or SE 1200/90. All the cases showed various degrees of the mass effect.

Inflammation (16 cases)

Eleven cases of cysticercosis, 4 cases of granulomatous lesions and 1 case of sphenoid sinus mucopyocele were studied.

Seven cases of the parenchymal and/or cisternal cysticercosis with typical cyst formation revealed same findings as those of CT on both SE 400/30 and SE 900/60, demonstrating round cysts of low intensity. The cysts appeared as high-intensity same as that of CSF on SE 1500/90 or SE 2000/80. Three cases of intraventricular cysticercosis in 4th ventricle could not be differentiated from the ventricular CSF on any pulse sequence. Intraventricu-

lar cysticercosis was correctly diagnosed with only metrizamide ventriculography or CT ventriculography, but not with MR. One case of cysticercosis with small calcified nodules and 4 non-calcified granulomatous lesions were seen as iso-intensity lesions on SE 400/30 and as high intensity area on SE 900/60 or SE 1200/90 images. Small calcific dot was not demonstrated on MR images. The granulomas were not differentiated from the surrounding edemas. One case of sphenoid mucopyocele revealed round homogeneous high intensity on both SE 400/30 and SE 900/60.

Demyelinating and degenerative diseases (28 cases)

This group consisted of 23 patients of white matter diseases including 11 cases with sequelae of acute carbon monoxide (CO) poisoning, 4 subcortical arteriosclerotic encephalopathy (SAE), 1 multiple sclerosis, 1 adrenoleukodystrophy, 1 radiation necrosis and 5 unknown white matter lesions. Five cases of Parkinsonism, Wilson's disease and olivopontocerebellar degeneration were also included here.

The white matter lesions appeared as bilateral diffuse and/or patchy areas on high-intensity in the periventricular region and centrum ovale on SE 900/60, SE 1200/90 or SE 2000/80. In 3 cases, the white matter lesions were not definitely shown on the SE 900/60 images, but clearly demonstrated on only SE 1500/90. The SE 400/30 and IR 1400/400/30 detected fewer lesions than did the SE 900/60 or SE 1200/90. The SE 900/60, SE 1200/90 or SE 2000/80 images also depicted the lesions as appearing larger and more coalescent than did the SE 400/30 and IR 1400/400/30. Of the 11 cases of CO poisoning sequelae, 5 patients had bilateral symmetrical areas of high intensity in white matter of periventricular and centrum ovale. Two patients showed bilateral symmetrical abnormalities in globus pallidus regions and six patients showed only diffuse atrophy.

Abnormalities of the basal ganglia or cortex in patients with degenerative diseases that predominantly affect the gray matter (Wilson's disease, Parkinsonisms, etc.) were seen as generalized or regional atrophy in MR, like CT studies.

Congenital Anomalies (3 cases)

Three cases including 1 Chiari malformation, ependymal cyst and 1 arachnoid cyst were studied. The mid-sagittal SE 400/30 image of the Chia

malformation depicted excellent features of downward displacement of 4th ventricle and cerebellar tonsils. The MR of both the arachnoid and the ependymal cyst demonstrated the same features of low intensity cyst as those of CT, but MR failed to demonstrate a tiny calcification in the ependymal cyst wall.

Miscellaneous (5 cases)

Two cases of hydrocephalus, 2 vertebral diseases and 1 scalp lipoma were studied. MR findings of the hydrocephalus was same as those of CT. Two disc diseases showed good anatomic details in midsagittal images on SE 400/30. The scalp lipoma is seen as high-intensity mass on SE 400/30.

Comparison of MR with CT

Of the 108 patients excluding 13 "normal" cases, 98 showed the lesions on both MR and CT. But in 10 patients, the lesions were missed or equivocally demonstrated on CT, but were well visualized on MR images. These consisted of 3 cases of white matter diseases (2 cases of CO poisoning and 1 SAE), 1 isodense subdural hematoma, 2 acute cerebellar infarctions, 1 brainstem tumor and 3 cases with unknown pathologies.

In 36 patients, the MR appeared superior to CT in the detection of the abnormalities, capability of demonstrating the extent of the lesions, contrast discrimination between normal and abnormal tissues, and giving other additional information (Table 2).

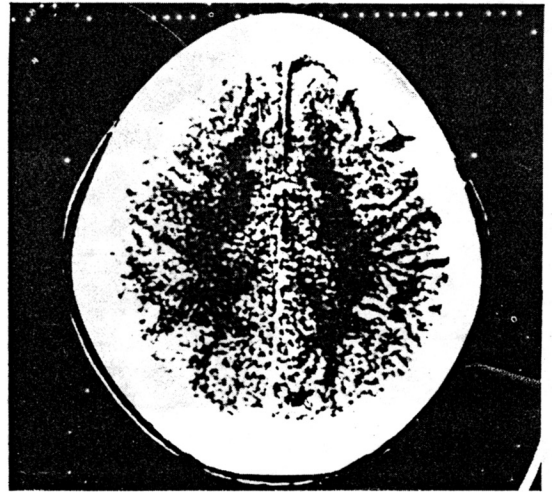
Table 2. MR better than CT

Diagnosis	Case No.
Demyelinating disease	10 (2)
CO poisoning	5 (1)
SAE	4 (1)
Multiple sclerosis	1
Cervical cord tumor (including Syringomyelia)	6 (2)
Chiari malformation	1
Foramen magnum meningioma	1 (1)
Brainstem tumor	2
Acute cerebellar infarction	2 (1)
AVM with hemorrhage	1
Cavernous hemangioma	1
Subdural hematoma (subacute)	2
Supratentorial glioma	1
Unknown	7
Normal	2
Total	36

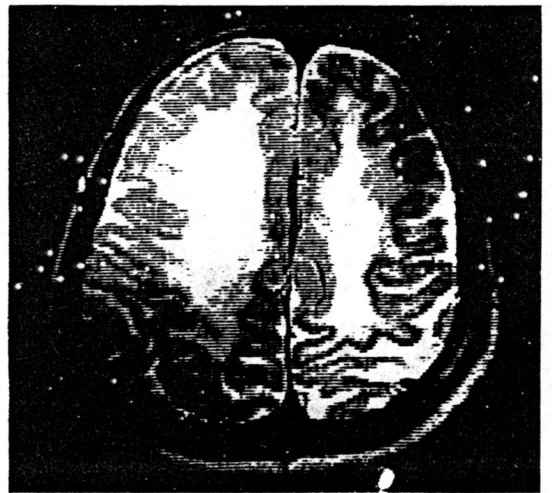
* No. in parenthesis: No. studied with 2.0T unit.

Periventricular white matter lesions were much better demonstrated in 5 cases with CO poisoning, 4 cases with SAE and 1 case of multiple sclerosis on SE 900/60, SE 1200/90, or SE 2000/80 images, in which CT showed no lesions or subtle low densities in the periventricular white matters (Fig. 1). The MR images also revealed wider extents of the lesions and more distinct contrast between normal and abnormal areas.

The MR of 6 out of 7 cervical cord tumors demon-



(A)



(B)

Fig. 1. Interval form of acute carbon monoxide (CO) poisoning. The CT (A) reveals no abnormality, while MR (SE 2000/80) (B) demonstrates extensive high signal intensity in white matter of centrum ovale bilaterally. MR image with 2.0T unit.



(A)

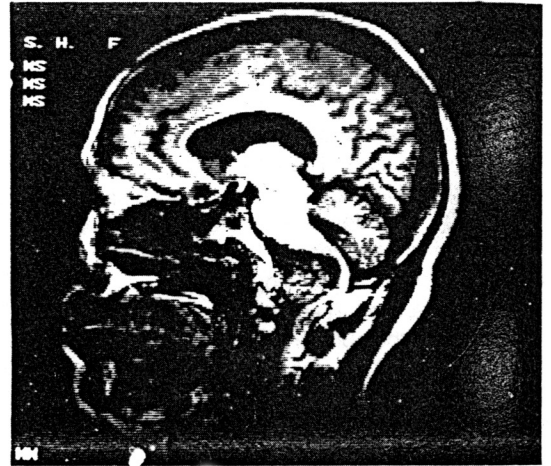


(B)

Fig. 2.



(A)



(B)

Fig. 3. Foramen magnum meningioma. The axial post-contrast CT image (A) shows round mass of high density in center of foramen magnum.

It is impossible to differentiate whether it is intra-axial or extra-axial mass.

But mid-sagittal MR image (IR 1500/700/30) (B) shows nice demonstration of the anatomic relationship between the brainstem and the tumor.

The meningioma of low signal intensity displaces the medulla and upper cervical cord posteriorly.

Fig. 2. Astrocytoma in cervical and thoracic spinal cord. The axial image of metrizamide CT (A) shows enlargement of spinal cord with syrinx cavity which was shown as high density of contrast media accumulation. The mid-sagittal image of MR (SE 400/30) (B) demonstrates enlargement of entire cervical and upper thoracic spinal cord which contains low signal intensity of syrinx cavity in upper thoracic level. Note excellent visualization of spinal cord in sagittal plane.

strated syrinx cavities within the spinal cord clearly in the sagittal section of SE 400/30, while metrizamide myelography and immediate CT demonstrated only widening of the cord but delayed CT showed the syrinx cavities in most cases (Fig. 2).

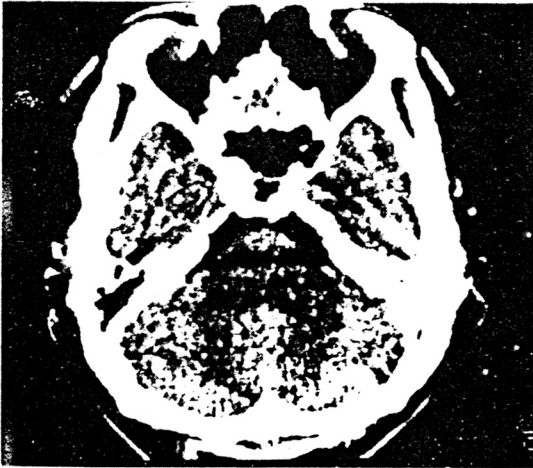
In each case of Chiari malformation and foramen magnum meningioma, MR also delineated much better anatomic details and relationship in midsagittal images than CT (Fig. 3).

Two brainstem tumors and 2 acute cerebellar infarctions could not be adequately evaluated with CT because of beam hardening artifacts while these lesions were readily detected with SE 900/60 or SE

2000/80 images (Fig. 4).

In one case of intracerebral hemorrhage secondary to rupture of the AVM MR showed multiple linear and tortuous vascular shadows of low intensity indicating high-flow AVM in area of the hematoma, which was not identified on CT. One case of the cavernous hemangioma also demonstrated curvilinear vascular shadows within the mass, which was not seen on CT.

In one CT-isodense subdural hematoma MR taken several days after CT showed bilateral crescentic areas of bright intensity over the parietal con-

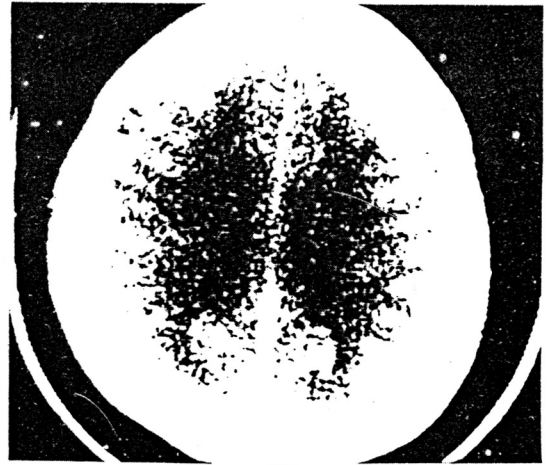


(A)



(B)

Fig. 4. Brainstem tumor. The post-contrast CT (A) shows no apparent abnormality. But T2 weighted SE image of MR (B) reveals high signal intensity mass in left side of pons and left brachium pontis area.



(A)



(B)

Fig. 5 Bilateral isodense subdural hematoma. The CT scan (A) reveals no apparent abnormal density in parietal convexity, while MR (SE 900/60) image (B) shows crescent shaped subdural hematoma of high signal intensity over the parietal convexity on both sides.

vexity on SE 900/60 images (Fig. 5). In a case with both intracerebral and subdural hematomas the CT density of the hematoma was high on 2 weeks after trauma, which became isodense in 4 weeks follow-up CT. But MR in 4 weeks after trauma demonstrated high intensity of hematomas on both SE 400/30 and SE 900/60 images.

One supratentorial glioma and 7 unknown pathologies demonstrated wider and more obvious extents of lesions with MR than with CT.

In two cases with suspicious abnormalities of low density in middle and posterior cranial fossas, respectively, on CT, SE 400/30 and SE 900/60 images demonstrated quite normal appearance. Suspicious low density on CT was thought to be due to beam hardening artifacts.

CT was more specific and superior to MR in 12 patients (Table 3). Although MR revealed some abnormalities in these patients, the appearance was not specific.

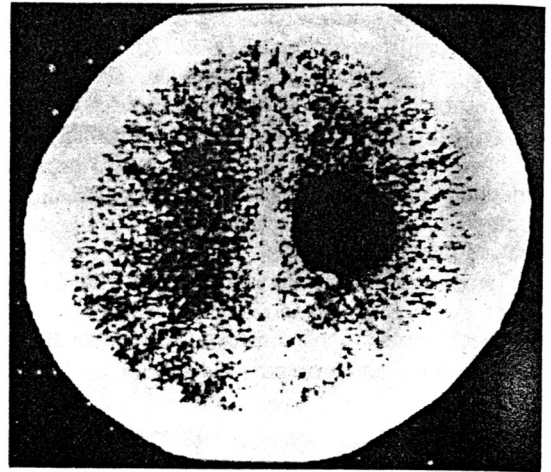
Table 3. CT better than MR

Diagnosis	Case No.
Small calcification	3
Cysticercosis	1
Granuloma (sparganosis)	1
Ependymal cyst	1
Inflammatory granuloma	3
Meningioma	2
Suprasellar enhancing mass	1
Acute hematoma	2
EDH	1
ICH	1
Unknown	1
Total	12

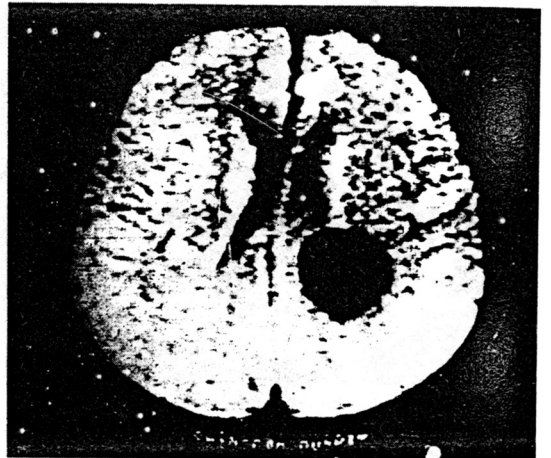
Small calcification in 1 cysticercosis, 1 ependymal cyst and 1 granuloma (sparganosis) was not seen on MR (Fig. 6).

In three cases of inflammatory granuloma, the granulomas could be separated from the surrounding low density of edema on contrast-enhanced CT, but not on MR (Fig. 7).

Two meningiomas were demonstrated much better with CT (Fig. 8). MR showed only subtle abnormality with poor contrast between normal tissue and tumor mass in meningiomas. Similarly, one suprasellar enhancing mass on CT also showed lower contrast with MR images.



(A)



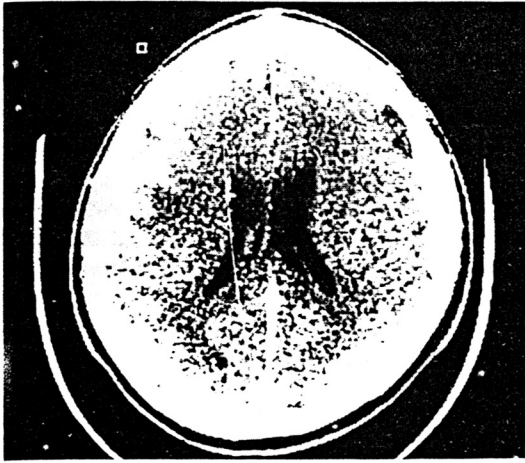
(B)

Fig. 6. Ependymal cyst. Both CT (A) and MR (SE 400/30) (B) images reveal round cystic mass of low density in left deep parietal lobe. But a small calcification was seen at posterior wall of the cyst on only CT, but not on MR.

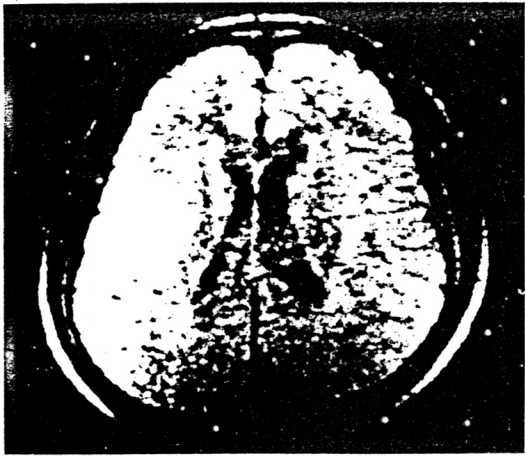
Acute hematomas were more obviously demonstrated with CT. In one case of acute basal ganglia hematoma and 1 epidural hematoma, the MR intensity of the hematoma appears to be slightly higher or almost same as the brain parenchyma in SE 400/30 images. In epidural hematoma, a curvilinear line of low intensity was seen along its medial border, indicating displaced dura.

Mass effect was equally seen with both MR and CT.

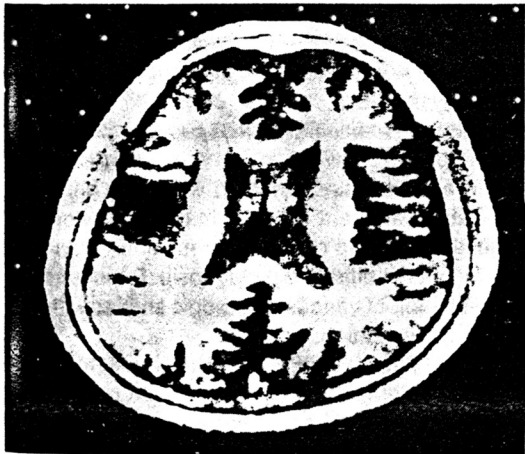
MR and CT provided equivalent information in remaining patients; In these patients MR gave no additional information to CT.



(A)

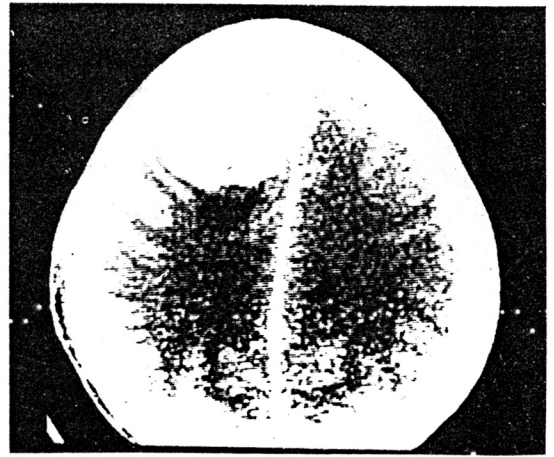


(B)



(C)

Fig. 7



(A)



(B)

Fig. 8. Meningioma. The post-contrast CT (A) reveals well-defined round mass with homogeneous enhancement at right frontal convexity. On MR (SE 1200/60) (B) image, the contrast between the tumor and normal tissue is much less distinct.

Fig. 7. Inflammatory granuloma. The post-contrast CT (A) reveals a small round enhancing nodule at right temporo-parietal cortex with surrounding edema of low density. The MR images show ill-defined high signal intensity and low signal intensity at right temporo-parietal lobe in T2 weighted SE (B) and T1 weighted IR (C) images, retrospectively. The granuloma could not be separated from the surrounding edema on MR images.

DISCUSSION

Our experience, although limited, suggests that cerebral MR imaging has considerable diagnostic potential, with several advantages over CT already apparent, but certain limitations exist at the present stage of development.

The superior sensitivity of MR has been reported previously in the case of demyelinating disease (Brant-Zawadzki et al., 1983; Bradley et al., 1984; Sheldon et al., 1985). In our series MR proved to be significantly more sensitive in the detection of periventricular white-matter lesions, i.e., CO poisoning, multiple sclerosis and SAE, though some patients did not show good spatial resolution in SE 900/60 or SE 1200/90.

The depiction of brain anatomy and pathologies with MR is superior to that offered by CT in regions where beam-hardening artifact occurs on CT images (Bydder et al., 1982; Bradley et al., 1984); MR better demonstrated tumors, infarcts, and gliosis of the brainstem and cerebellum, where CT was limited by beam hardening artifacts (Bradley et al., 1984).

At this stage, MR imaging is also the procedure of choice for evaluating the crano-vertebral junction, and cervical spinal cord (particularly syringomyelia and tumor) (Han et al., 1983; Hawkes et al., 1983; Lee et al., 1985; Norman et al., 1984). MR proved to be at least as accurate as delayed metrizamide CT in the diagnosis of intramedullary cavities that result in spinal cord enlargement, but it is less sensitive in detecting cavities within normal-sized or diminished spinal cords. The syringes associated with tumor is difficult to distinguish from uncomplicated syringomyelia in some cases (Lee et al., 1985).

Extracerebral hematomas usually show characteristic CT findings that are virtually diagnostic. However, diagnosis of isodense subdural hematomas can be problematic using CT. MR easily resolves this problem by revealing not only an abnormal fluid collection but its entire extent over the cerebral convexity (Young et al., 1983; Han et al., 1984). A previous report on MR imaging stated that acute extracerebral collections appear as bright intensities on SR (saturation recovery) and IR images, representing short T1 relaxation times (Young et al., 1983). However, in our case of an acute epidural hematoma the hematoma showed up as an iso-signal intensity. The MR diagnosis of acute epidural hematoma was made by both mass

effect and medially displaced dura mater of low intensity. The same findings as ours in epidural hematoma were previously reported by Han et al (Han et al., 1984), who suggested that as the aging extracerebral blood undergoes organization the T1 relaxation time is reduced while the T2 relaxation time remains constant. The accuracy and time course of CT changes in intracerebral hemorrhage are well established (Dolinskas et al., 1977); However, MR of the acute hematoma showing central area of iso-intensity with a rim of high intensity at the periphery is of interest. It is suggested that stages of organization and resolution of intracerebral hemorrhage at the periphery may have shorter T1 (high intensity at rim) than blood clots at the center (isointensity at center).

In cerebral infarction within the cerebral hemispheres MR appearances generally paralleled those of CT; MR appears not superior to CT in specific diagnosis of cerebral infarction (Bydder et al., 1982).

Hydrocephalus was equally well seen with MR and CT, although the periventricular CSF migration is usually better defined by MR (Bydder et al., 1982). The cerebral aqueduct may occasionally be seen in MR.

While localized or generalized cerebral atrophy is equally well demonstrated with MR and CT, the absence of artifact in the posterior fossa enables atrophy of the cerebellum to be seen more clearly.

In SE 400/30 images (partially T1 weighted image), many pathologies including most of the tumors, infarctions, inflammations, demyelinating diseases and edema appear as low intensities due to long T1, while these show high intensities in SE 1200/60 due to long T2. These intensities is relatively non-specific, and other factors need to be considered in order to distinguish different types of pathology (Bydder et al., 1982). The CT findings were also non-specific in most cases, but accumulated experience over the years in visualization of certain abnormalities, coupled with their anatomic distribution, appearance after intravenous contrast administration, and clinical presentation, often permits a concise differential diagnosis. Experience in differentiation of various pathologic entities with MR is now accumulating.

It is well known that the superior signal to noise-ratio at the higher magnetic field can be used effectively to image thinner sections at finer spatial resolution without excessive examination time (Bilaniuk et al., 1984). Although our clinical experi-

ence with 2.0T superconducting system is very limited to small numbers of patients, and images were obtained at early developing stage, it proved that the 2.0T images revealed both the anatomy and abnormalities in much greater detail than did 0.15T images. The high field studies revealed the relationship and the effect on the adjacent structures much better. The vascular structures are best demonstrated. The ability to achieve a good signal to noise ratio and to obtain thin sections (5mm) allowed the demonstration of tracts and nuclei in the brain stem. But these remains to be further evaluated.

CT was able to provide a more specific diagnosis of meningioma, due to the presence of calcification, dense enhancement and hyperostosis; however, MR did at least large tumors (Bradley et al., 1984). CT was also better able to separate tumor from edema due to contrast agents which defined breakdown of the blood-brain barrier (Bradley et al., 1984). Currently paramagnetic contrast agents could give MR the same capability (Graif et al., 1985; Claussen et al., 1985). Patients who are likely to move are much better evaluated in a few seconds by CT than in a few minutes by MR; this includes not only those with acute trauma but also the elderly and the very young. Extremely ill patients on a respirator or pacemaker cannot be examined with MR, since these devices cannot function in a strong magnetic field.

Our present study is by no means a rigorous comparative study of MR versus CT. The lesions in most cases were known to be present on CT before MR study, and no double blind study was used. Since MR imaging techniques have been continually improved and refined, this report is meant only to define the capabilities of MR at the present time and to suggest those areas in which it might complement a CT study. Whether it can totally supplant CT in some of these disease entities remains to be fully determined.

REFERENCES

- Bilaniuk LT, Zimmerman RA, Wehrli FW, et al.: *Cerebral magnetic resonance: Comparison of high and low field strength imaging. Radiology 153:409-414, 1984.*
- Bradley WG, Waluch V, Yadley RA, Wycoff RR: *Comparison of CT and MR in 400 patients with suspected disease of the brain and cervical spinal cord. Radiology 152:695-702, 1984.*
- Brant-Zawadzki M, Davis PL, Crooks LE, et al.: *NMR demonstration of cerebral abnormalities; Comparison with CT. AJNR 4:117-124, 1983.*
- Bydder GM, Steiner RE, Young IR, et al.: *Clinical NMR imaging of the brain 140 cases. AJR 139:215-236, 1982.*
- Claussen C, Laniado M, Schoerner W, et al.: *Gadolinium-DTPA in MR imaging of glioblastomas and intracranial metastases. AJNR 6:669-674, 1985.*
- Dolinskas CA, Bilaniuk LT, Zimmerman RA, et al.: *Computed Tomography of intracerebral hematomas. I. Transmission CT observations on hematoma resolution. AJR 129:681-688, 1977.*
- Graif M, bydder GM, Steiner RE, et al.: *Contrast enhanced MR imaging of malignant brain tumors. AJNR 6:855-862, 1985.*
- Han JS, Kaufman B, Yousef SJ, et al.: *NMR imaging of the spine. AJNR 4:1151-1159, 1983.*
- Han JS, Kaufman B, Alfidi RJ, Yeung HN, et al.: *Head trauma evaluated by magnetic resonance and computed tomography; A comparison. Radiology 150:71-77, 1984.*
- Hawkes RC, Holland GN, Moore WS, et al.: *Craniovertebral junction pathology; Assessment by NMR. AJNR 4:232-233, 1983.*
- Lee BCP, Zimmerman RD, Manring JJ, et al.: *MR imaging of syringomyelia and hydromyelia. AJNR 6:221-228, 1985.*
- Norman D, Mills CM, Brant-Zawadzki M, et al.: *Magnetic resonance imaging of the spinal cord and canal; Potentials and limitations. AJNR 5:9-14, 1984.*
- Sheldon JJ, Siddharthan R, Tobias J, et al.: *MR imaging of multiple sclerosis; Comparison with clinical and CT examinations in 74 patients. AJNR 6:683-690, 1985.*
- Young IR, Bydder GM, Hall AS, et al.: *Extracerebral collections; Recognition by NMR imaging. AJNR 4:833-834, 1983.*